CHEMISTRY
A EUROPEAN JOURNAL

DOI: 10.1002/chem.201001280

Strategic Synthesis of Hierarchical TiO_2 Microspheres with Enhanced Photocatalytic Activity

Zhaoke Zheng,[a] Baibiao Huang,*[a] Xiaoyan Qin,[a] Xiaoyang Zhang,[a] and Ying Dai[b]

Synthesis and characterization of one-dimensional structures have attracted much attention due to their potential applications in a variety of fields.[1–3] Among the one-dimensional nanomaterials reported, special attention has been directed to TiO_2 due to its unique functional properties such as increased photocorrosion resistance,[4] high photoconversion efficiency,[5–7] and its suitability as a material for purification of water and air.[8–10] Recently, hierarchical inorganic materials have attracted significant scientific and technological interest in functional materials synthesis. Such hierarchical structures proved to be very efficient when using them for practical applications such as water treatment,[11] electrodes for lithium batteries, dye-sensitized solar cells, and catalyst supports.[12] More importantly, the hierarchical structure possesses good light-scattering properties which are expected to provide more efficient light harvesting. Thus, for use as a practical catalyst, hierarchical TiO_2 materials produced from one-dimensional building blocks are highly desirable.

There have been extensive studies to explore approaches to the synthesis of hierarchical materials, such as chemical vapor deposition methods and solution-phase chemical routes. Among them, the assembly of 1D or 2D nanoscale building blocks into 3D hierarchical superstructures is the most common synthetic route. However, this route usually requires catalysts, and expensive and even toxic templates or surfactants to complete the assembly process.[13] Moreover, assembly of 1D building blocks to hierarchical materials with a particular morphology is generally more difficult.

[a] Z. Zheng, Prof. Dr. B. Huang, X. Qin, Prof. X. Zhang
State Key Lab of Crystal Materials
Shandong University, Jinan 250100 (China)
Fax: (+86) 531-8836-5969
E-mail: bbhuang@sdu.edu.cn

[b] Prof. Dr. Y. Dai
School of Physics
Shandong University, Jinan 250100 (China)

Supporting information for this article is available on the WWW under http://dx.doi.org/10.1002/chem.201001280.

Different from the conventional method for hierarchical materials, herein we report that a strategic synthetic method leads to hierarchical TiO_2 microspheres (HTM) with a 1D structure. In our synthetic strategy, primary TiO_2 microspheres (PTM) were first synthesized by a simple alcohothermal method. Then, under alkali hydrothermal treatment, these primary microspheres (precursors) transformed into HTM with a hierarchical nanotubular structure. After annealing, these HTM samples exhibit a porous dendritic structure. This may provide a facial route to produce hierarchical TiO_2 with a particular matrix morphology.

The scanning electron microscopy (SEM) images of the PTM precursors show that they have a smooth surface and are produced from TiO_2 nanoparticles (Figure 1a and b). After alkali hydrothermal treatment and acid washing, hierarchical microspheres with diameters in the range of 4–6 μm were formed (Figure 1c). The higher magnification SEM and TEM images of the HTM sample revealed that the microspheres are produced from TiO_2 nanotubes with diameters of $\approx$10 nm and lengths of several micrometers (Figure 1d). These nanotubes wrapped around each other to form mesoporous microspheres.

Once exposed to alkali hydrothermal treatment, the Ti–O–Ti bonds in the TiO_2 nanoparticles of the PTM were broken to form Ti–O–Na.[14] Single- or multilayered titanate nanosheets were formed in situ, then these nanosheets converted into nanotubes, either by scrolling (rolling-up) single-layer nanosheets[15] or by curving (wrapping) of conjoined nanosheets.[16] More importantly, the as-synthesized HTM sample retains the original sphere morphology of the PTM precursor. Both anatase and titanate contain zigzag ribbons of TiO_6 octahedra that share four edges with the others, and the common structural features make the phase transition from anatase to titanate relatively easy.[17] Therefore, the original sphere morphology could be retained. Unlike conventional hierarchical material synthesis, in which it is difficult to control the morphology of the finally assembled material, this method is rather convenient to control the morphology of the hierarchical products by varying the presynthesized precursor.

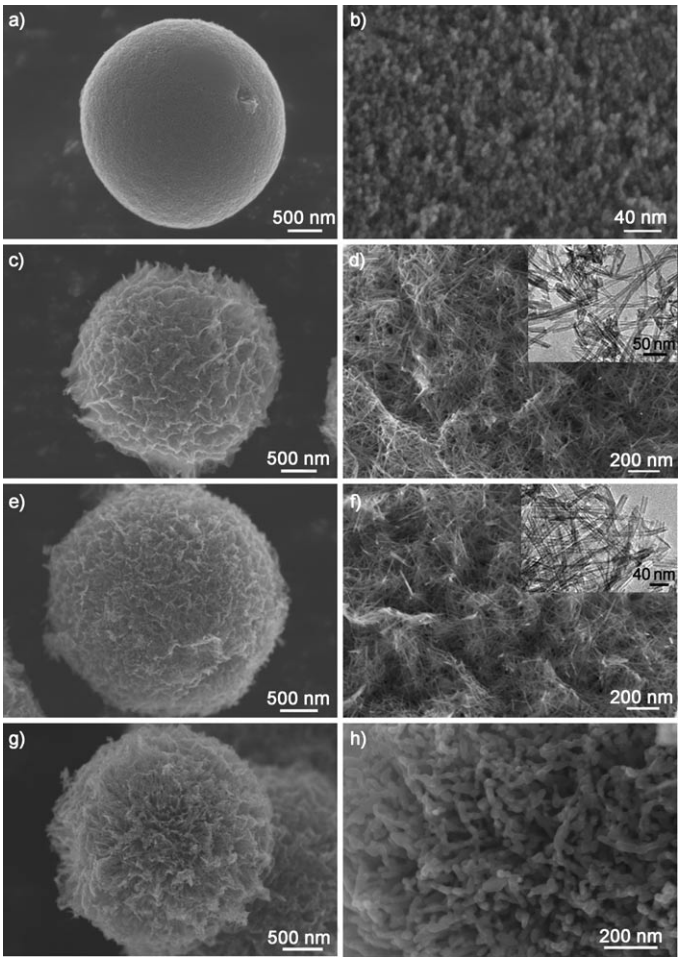

Figure 1. SEM and TEM (inset) images of PTM (a and b) and the as-prepared HTM and calcined HTM samples (c and d) at 400 (e and f) and 600 °C (g and h).

The HTM sample after calcination at 400 °C still retained the hierarchical nanotubular structure (Figure 1 e and f). The spaces between the adjacent nanotubes and the inner space of the nanotubes can act as a light-transfer path for introducing incident photon flux onto the inner surface of microspheres, and enhances photocatalytic activity.[18] More importantly, the open mesoporous structure makes the hierarchical microsphere a potential candidate for concurrent membrane filtration with photocatalysis, which is widely used in advanced photocatalytic membrane water-treatment engineering. After calcination at 500 °C, the nanotubular structure is destroyed and the nanotubes transform into branchlike nanorods (see Figure S2 e and f in the Supporting Information). It is indicated that titanate nanotubes are unstable at temperatures above 400 °C, and this is in agreement with the results reported before.[19] Upon further increase of the calcination temperature to 600 °C, the microspheres present open dendritic structures (Figure 1 g and h).

The X-ray diffraction (XRD) pattern (see Figure S3 a in the Supporting Information) shows that the presynthesized PTM sample is a pure anatase phase of TiO_2 with a lattice constant $a = 3.7852$ Å (JCPDS No. 21-1272). After alkali hydrothermal treatment at 150 °C for 24 h, the anatase PTM completely transformed into sodium titanate (see Figure S3 b in the Supporting Information).[20] The XRD pattern of the finally formed HTM samples show vague peaks in anatase phase (see Figure S3 c in the Supporting Information),[21] and the anatase (with a longer c axis) has been reported to be the preferred phase in TiO_2 nanotubes.[22] Figure S4 (in the Supporting Information) shows the XRD pattern of the HTM samples after calcination at different temperatures. With calcination at 400 °C the HTM transformed into a well-crystallined anatase phase of TiO_2. Upon increasing the calcination temperature to 600 °C, a small peak at 27.4°, corresponding to the (110) plane diffraction of rutile TiO_2 (JCPDS No. 21-1276) appeared. This indicates that the phase transformation temperature of anatase to rutile is at about 600 °C, which is in good agreement with that reported by Yu et al.[23]

The open porous structure of the HTM samples was confirmed by the nitrogen adsorption-desorption experiment. Figure 2 a shows the typical isotherms of N_2 adsorption onto HTM samples after calcination at different temperatures.

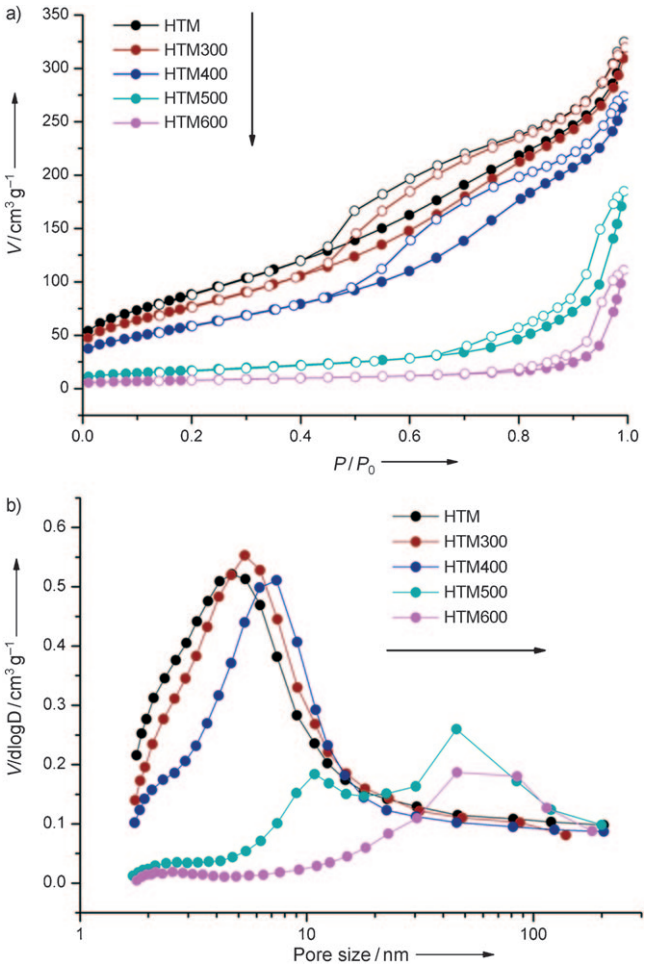

Figure 2. a) Nitrogen adsorption–desorption isotherm (● = adsorption, ○ = desorption) and b) pore-size distribution curves of HTM samples before and after calcination at different temperatures.

All these isotherms exhibit a clear hysteresis loop, indicating that the products are mainly mesoporous.[21] After calcination below 400 °C, the adsorption–desorption isotherms of the samples appear to be similar, indicating that the pore structure did not change much under low-temperature calcination. However, upon further increase of the calcination temperature to 500 °C, the shape of the hysteresis loop clearly changes. The isotherm of the sample calcined at 600 °C is similar to that calcined at 500 °C, indicating that HTM500 and HTM600 samples have similar pore structures. The Barrett–Joyner–Halenda (BJH) method was employed to analyze the pore-size distribution and the results are shown in Figure 4b. After calcination below 400 °C, the pore-size distribution of the sample was similar, which is in good agreement with the results of N_2 adsorption–desorption isotherms. The slight shift to the right means that the pore size gradually increases with the calcination temperature. At 500 °C, the pores range from 2 to 10 nm decreased abruptly. It can be concluded that the original pore structure of HTM is destroyed when the calcination temperature is over 500 °C.

The pore structures calculated according to the adsorption data are summarized in Table 1. The as-prepared HTM sample shows a very large specific surface area of

Table 1. The effects of calcination temperatures on the pore structures of HTM samples.

Calcination temperatures [°C]	S_{BET} [$m^2 g^{-1}$]	Pore volume [cm^3]	Average pore size [nm]
as prepared	325.3	0.50	6.18
300	284.0	0.49	6.96
400	215.8	0.42	7.85
500	61.1	0.29	18.71
600	27.4	0.17	25.05

325.3 $m^2 g^{-1}$ and a high pore volume of 0.50 $cm^3 g^{-1}$. After calcination at 400 °C, the specific surface area and pore volume decreased to 215.8 $m^2 g^{-1}$ and 0.42 $cm^3 g^{-1}$, respectively. When the sample was calcined at 500 °C, the specific surface area decreased drastically to 61.1 $m^2 g^{-1}$, and the average pore size increased sharply to 18.71 nm. This is due to the collapse of the nanotubular structure. Yu et al. have reported that at 600 °C, the specific surface area of their hierarchical mesoporous titania decreased drastically to 0.8 $m^2 g^{-1}$ and the pore volume became very small.[23] However, at 600 °C, the specific surface area and pore volume of our sample retain a relative high value, 28.4 $m^2 g^{-1}$ and 0.17 $cm^3 g^{-1}$, respectively. Clearly, the mesoporous structure of our products shows higher thermal stability.

The UV/Vis diffuse reflectance spectra of HTM400 and commercially available Degussa P25 are compared in Figure S5 (in the Supporting Information). HTM400 has a stronger adsorption in the UV region than Degussa P25, which may be due to the good light-scattering property of the unique hierarchical nanotubular structure. Therefore, this hierarchical nanotubular structure is expected to provide more efficient light harvesting and an enhanced photocatalytic activity.

The photocatalytic activity of hierarchical TiO_2 microspheres was examined by probing the photocatalytic decomposition of methyl orange (MO) as a function of irradiation time (Figure 3).[24] The concentration of MO in the solution

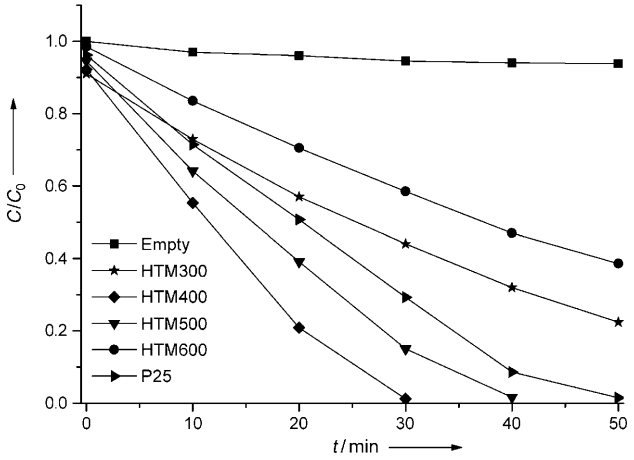

Figure 3. Photodegradation of methylene orange (20 mgL^{-1}) over different samples under full Xe arc light irradiation.

slightly decreases while it is kept in the dark owing to the adsorption of MO on the catalysts. The sample calcined at 400 °C shows the highest photocatalytic activity, which may be due to the high surface area of nanotubular structure and good crystallinity. With an increase in the calcination temperature to 500 °C, the photocatalytic activity of the sample is still higher than that of Degussa P25. This is due to the open porous structure of the HTM500. The poor crystallinity for HTM300 and low surface area for HTM600 explain the relative lower photocatalytic activity of these two samples.

Owing to the nanotubular structure and the open porous networks, the HTM400 sample may have promising applications in advanced water treatment combined with concurrent filtration with photocatalysis. Figure 4a shows the schematic diagram of water filtration treatment with photocatalysis. Phenol and Cr^{VI} were used as probe molecules.[25] Under UV irradiation, the conversion of phenol oxidation and chromium reduction was 57 and 97%, respectively (Figure 4b). Clearly, the larger particle size of the microspheres avoids dense packing of the catalyst, which permits facile fluid transport; the nanotubular and mesoporous structures provide an efficient transport pathway to their interior voids, which could effectively improve the contact area in advanced water treatment.

In addition to the above water-treatment applications, noble metals can also be easily loaded on the surface of our samples, and the nanotubular structure and open porous networks provide efficient supports for loading of Au and Ag nanoparticles. As shown in Figure 5, noble-metal nanoparticles (10–25 nm) have been evenly deposited on the sur-

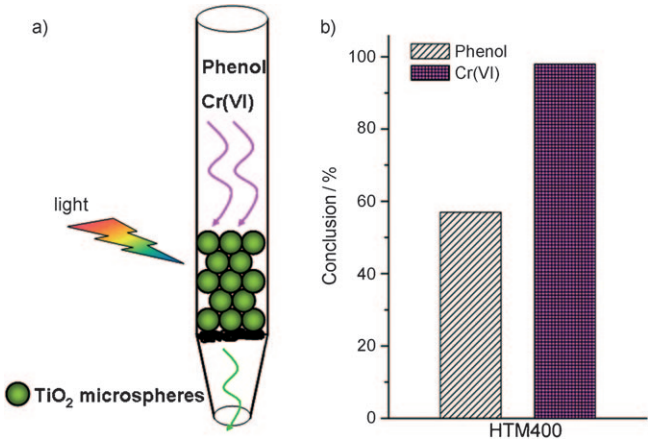

Figure 4. a) Schematic diagram of water filtration treatment with photocatalysis and b) photocatalytic activity of HTM400 in phenol-oxidation and chromium-reduction reactions.

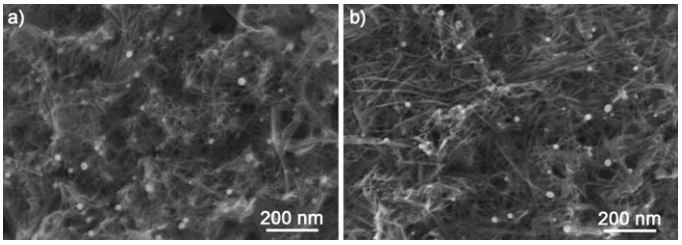

Figure 5. SEM images of HTM400 loaded with a) Au and b) Ag.

faces of the HTM400 sample. Plasma resonance peaks of Au and Ag are observed at approximately 543 and 459 nm, respectively (see Figure S7 in the Supporting Information). Such noble-metal modified hierarchical TiO_2 microspheres may be efficient visible-light photocatalysts owing to the surface plasma resonance,[26–28] and could be used in various fields such as organic waste treatment and disinfectants for filtering water.

In summary, we have developed a facile method of synthesizing hierarchical TiO_2 microspheres with nanotubular and dendritic structure. Owing to the high surface area and open porous networks, the synthesized TiO_2 microspheres exhibit a superior photocatalytic activity, and are promising for practical applications such as solar cells, catalyst supports, and water-treatment engineering. This method provides a facile strategy to the synthesis of hierarchical materials with a particular matrix morphology.

Experimental Section

Primary TiO_2 microspheres: PTM were prepared on the basis of an alcohothermal reaction of the mixture of $Ti(OBu)_4$, absolute ethanol, deionized water, and sulfuric acid of AR grade. In a typical procedure, $Ti(OBu)_4$ (5.1 g) was mixed with absolute ethanol (75 mL) under vigorous stirring. After, sulfuric acid (0.33 mL, 98%) and deionized water (0.3 mL) were added. The resulting solution was transferred to a dried Teflon autoclave, and then kept at 180 °C for 4 h. After being cooled to room temperature, the white precipitate was collected, washed with ethanol for several times, and dried at 40 °C.

Hierarchical TiO_2 microspheres

General procedure: HTM were synthesized by alkali hydrothermal methods. In a typical procedure, PTM (0.5 g) were mixed with a 10 M NaOH aqueous solution (50 mL), followed by hydrothermal treatment at 150 °C in a Teflon autoclave for 24 h. Then, the filtered sample was dispersed into a 0.1 M HCl aqueous solution (600 mL) for 12 h, and washed thoroughly with deionized water. The powder was collected and dried at 60 °C to give the HTM. By annealing the HTM at different temperatures range from 300 to 600 °C for 1 h, anatase TiO_2 microspheres were obtained and named as HTM300, HTM400, HTM500, and HTM600.

Synthesis of an Au-loaded HTM400 sample: An Au-loaded HTM400 sample was prepared by a photodeposition method. An aqueous suspension containing a sample of HTM400 (200 mg) and $HAuCl_4{\cdot}4H_2O$ (4.2 mg>) was irradiated with a 300 W Xe arc lamp for 0.5 h, before the purple precipitate was collected and dried at 40 °C. The loading amount of noble metal was 1wt%.

Synthesis of an Ag-loaded HTM400 sample: An Ag-loaded HTM400 sample was prepared by the same procedure as above except that $HAuCl_4{\cdot}4H_2O$ was replaced by $AgNO_3$ (3.1 mg). The loading amount of noble metal was 1wt%.

X-ray diffraction: XRD patterns were obtained by using a Bruker D8 advanced X-ray powder diffractometer with $Cu_{K\alpha}$ radiation ($\lambda = 1.5418$ Å). The morphologies of the samples were examined by SEM (Hitachi S-4800 microscope) and HRTEM (JEOL JEM-2100). The surface areas of the TiO_2 microspheres were measured by using the Brunauer–Emmett–Teller method with a Builder 4200 instrument at liquid nitrogen temperature. The pore volume and the pore-size distribution of the TiO_2 microspheres were derived from the absorption branch of the absorption–desorption isotherms by using the Barrett–Joyner–Halenda method. The diffuse reflectance spectra were measured on a Shimadzu UV 2550 UV/Vis spectrophotometer.

Photocatalytic properties: MO dye was chosen to evaluate the photocatalytic properties of the TiO_2 microspheres. In a typical reaction, 0.1 g of samples were dispersed in a Pyrex glass reactor (with the cross section of 30 cm^2 and the height of 5 cm) containing 100 mL MO solutions with a concentration of 20 mg L^{-1}. The optical system for detecting the catalytic reaction consisted of a 300 W Xe arc lamp (PLS-SXE300, Beijing Trusttech), and the degradation of MO dye was monitored by UV/Vis spectroscopy (UV-7502PC, Xinmao, Shanghai). Water filtration treatment with photocatalysis was carried out on a laboratory-scale test unit (glass tube with diameter of 0.7 cm). The catalyst (0.5 g) was filled into the tube with absorbent cotton as the supporting layer. An aqueous solution containing phenol (6.0×10^{-4} M) and $K_2Cr_2O_7$ (4.0×10^{-4} M) flowed through the catalyst under UV irradiation. The concentration and conversion of phenol and Cr^{VI} were analyzed by using a UV spectrophotometer (UV-7502PC, Xinmao, Shanghai) at their characteristic wavelengths (phenol = 270 nm, Cr^{VI} = 350 nm).

Acknowledgements

This work was financially supported by research grants from the National Basic Research Program of China (No. 2007CB613302) and the National Natural Science Foundation of China (Nos. 20973102, 50721002, and 10774091).

Keywords: nanostructures · nanotubes · photocatalysis · porosity · titanium

[1] S. Iijima, *Nature* **1991**, *354*, 56–58.

[2] C. N. R. Rao, B. C. Satishkumar, A. Govindaraj, M. Nath, *ChemPhysChem* **2001**, *2*, 78–105.
[3] Z.-G. Zhao, M. Miyauchi, *Angew. Chem.* **2008**, *120*, 7159–7163; *Angew. Chem. Int. Ed.* **2008**, *47*, 7051–7055.
[4] M. R. Hoffmann, S. T. Martin, W. Choi, D. W. Bahnemann, *Chem. Rev.* **1995**, *95*, 69–96.
[5] N. Vlachopoulos, P. Liska, J. Augustynski, M. Graetzel, *J. Am. Chem. Soc.* **1988**, *110*, 1216–1220.
[6] P. Maggie, S. Karthik, Y. Sorachon, E. P. Haripriya, K. V. Oomman, K. M. Gopal, A. L. Thomas, F. Adriana, A. G. Craig, *J. Phys. Chem. B* **2006**, *110*, 16179–16184.
[7] R. K. Karn, O. N. Srivastava, *Int. J. Hydrogen Energy* **1999**, *24*, 27–35.
[8] X. W. Zhang, A. J. Du, P. F. Lee, D. D. Sun, J. O. Leckie, *Appl. Catal. B* **2008**, *84*, 262–267.
[9] A. L. Linsebigler, G. Lu, J. T. Yates Jr. , *Chem. Rev.* **1995**, *95*, 735–758.
[10] S. P. Albu, A. Ghicov, J. M. Macak, R. Hahn, P. Schmuki, *Nano Lett.* **2007**, *7*, 1286–1289.
[11] J. H. Pan, X. W. Zhang, A. J. H. Du, D. D. Sun, J. O. Leckie, *J. Am. Chem. Soc.* **2008**, *130*, 11256–11257.
[12] S. Matsuda, *Appl. Catal.* **1983**, *8*, 149–165.
[13] W. S. Wang, L. Zhen, C. Y. Xu, L. Yang, W. Z. Shao, *Cryst. Growth Des.* **2008**, *8*, 1734–1740.
[14] T. Kasuga, M. Hiramatsu, A. Hoson, T. Sekino, K. Niihara, *Langmuir* **1998**, *14*, 3160–3163.
[15] B. D. Yao, Y. F. Chan, X. Y. Zhang, W. F. Zhang, Z. Y. Yang, N. Wang, *Appl. Phys. Lett.* **2003**, *82*, 281–283.
[16] D. V. Bavykin, V. N. Parmon, A. A. Lapkin, F. C. Walsh, *J. Mater. Chem.* **2004**, *14*, 3370–3377.
[17] H. Y. Zhu, X. P. Gao, Y. Lan, D. Y. Song, Y. X. Xi, J. C. Zhao, *J. Am. Chem. Soc.* **2004**, *126*, 8380–8381.
[18] Z. K. Zheng, B. B. Huang, X. Y. Qin, X. Y. Zhang, Y. Dai, M. H. Jiang, M.-H. Whangbo, *Chem. Eur. J.* **2009**, *15*, 12576–12579.
[19] H. Y. Zhu, Y. Lan, X. P. Gao, S. P. Ringer, Z. F. Zheng, D. Y. Song, J. C. Zhao, *J. Am. Chem. Soc.* **2005**, *127*, 6730–6736.
[20] E. Morgado Jr. , M. A. S. de Abreu, G. T. Moure, B. A. Marinkovic, P. M. Jardim, A. S. Araujo, *Chem. Mater.* **2007**, *19*, 665–676.
[21] C.-C. Tsai, H. Teng, *Chem. Mater.* **2004**, *16*, 4352–4358.
[22] Q. Zhang, L. Gao, J. Sun, S. Zheng, *Chem. Lett.* **2002**, 226–227.
[23] J. G. Yu, Y. R. Su, B. Cheng, *Adv. Funct. Mater.* **2007**, *17*, 1984–1990.
[24] P. Wang, B. B. Huang, X. Y. Qin, X. Y. Zhang, Y. Dai, J. Y. Wei, M.-H. Whangbo, *Angew. Chem.* **2008**, *120*, 8049–8051; *Angew. Chem. Int. Ed.* **2008**, *47*, 7931–7933.
[25] H. X. Li, Z. F. Bian, J. Zhu, Y. N. Huo, H. Li, Y. F. Lu, *J. Am. Chem. Soc.* **2007**, *129*, 4538–4539.
[26] P. Wang, B. B. Huang, X. Y. Zhang, X. Y. Qin, H. Jin, Y. Dai, Z. Y. Wang, J. Y. Wei, J. Zhan, S. Y. Wang, J. P. Wang, M.-H. Whangbo, *Chem. Eur. J.* **2009**, *15*, 1821–1824.
[27] P. Wang, B. B. Huang, Z. Z. Lou, X. Y. Zhang, X. Y. Qin, Y. Dai, Z. K. Zheng, X. N. Wang, *Chem. Eur. J.* **2010**, *16*, 538–544.
[28] Z. F. Zheng, J. Teo, X. Chen, H. W. Liu, Y. Yuan, E. R. Waclawik, Z. Y. Zhong, H. Y. Zhu, *Chem. Eur. J.* **2010**, *16*, 1202–1211.

Received: May 12, 2010
Published online: August 25, 2010

